Supporting Information

Fe(III) complex of biuret-amide based macrocyclic ligand as peroxidase enzyme mimic

By Chakadola Panda, Munmun Ghosh, Tamas Panda, Rahul Banerjee and Sayam Sen Gupta[a*]

Experimental Details:

Materials

All reagents were obtained from Sigma Aldrich and used without further purification unless indicated otherwise. N,N-dichloroformylmethylamine was obtained from ChemCollect, Gmbh. Solvents were dried and purified as described elsewhere[1]. **2** was synthesized as described in the literature[2].

Physical Measurements

^{1}H and ^{13}C NMR spectra were measured on Bruker(200MHz) spectrometer & these data are reported in δ(ppm) vs $(CH_3)_4Si$ with the deuterated solvent proton residuals as internal standards. Infrared spectra were obtained on a Perkin-Elmer FT-IR spectrum GX instrument . UV-visible spectra were taken on a Perkin-Elmer –λ35 spectro photometer fitted with a Perkin-Elmer Peltier with digital temperature controller. The temperature was set constant at 25 °C for all the experiments. ESI-MS was done on a Acquity Waters LC-MS. EPR spectrum was recorded on a Bruker EMX X-band spectrometr operating at a field modulation of 100 kHz, modulation amplitude of 2 G and microwave radiation power of 2 mW. The solid Fe(III) complex was taken in a quartz tube and the spectrum was recorded at 298 K. Electrochemical properties were investigated by cyclic voltammetry (CV) using an Autolab PGSTAT30 (Eco-Chemie) instrument in a conventional three-electrode test cell with platinum as the working electrode (WE), platinum wire as quasireference electrode (RE) and a platinum foil as a counter electrode(CE). The measurements were carried out using a solution of 1 mM of **1** in dry acetonitrile with 0.1 M $[n\text{-}Bu_4N]PF_6$ as the supporting electrolyte. All reversible couples were confirmed by a linear dependence of peak current vs. the square root of the scan rate over the range of 20-200 mV s^{-1}.

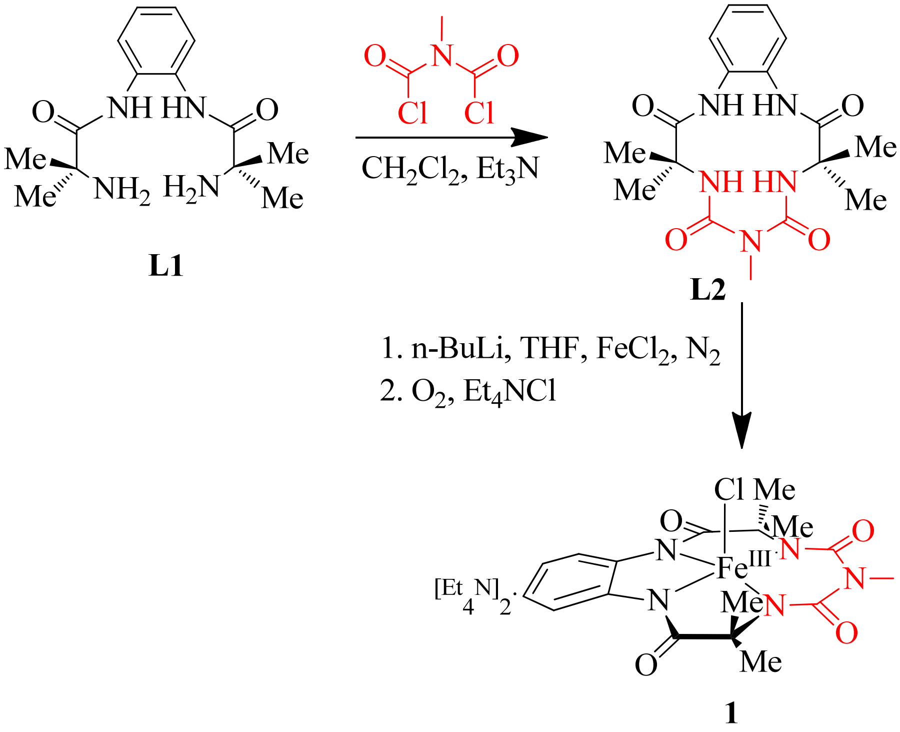

Scheme S1 : Synthetic scheme of biuret-amide macrocyclic ligand(**L2**) and its Fe^{III} complex(**1**)

N,N'-(1,2-phenylene)bis(2-amino-2-methylpropanamide) (**L1**) was synthesized as has been described before[2].

Synthesis of *3,3,6,9,9-pentamethyl-3,4,8,9-tetrahydro-1H-benzo[i][1,3,5,8,11]pentaazacyclotridecine-2,5,7,10(6H,11H)-tetraone* (**L2**)

Compound **L1** (500 mg, 1.79 mmol) was added to 50 mL dry CH_2Cl_2 with dry Et_3N (0.25ml, 1.79 mmol, 1 eq) and the resultant solution was transferred into an addition funnel. N,N-dichloroformylmethylamine (0.23 ml, 1.79 mmoles, 1eq) was diluted with 50 mL dry CH_2Cl_2 and was also transferred into another addition funnel. Both these solutions were added drop wise over a period of 1 hr into a 500 mL 3-necked round bottom flask containing 300 mL of dry CH_2Cl_2 at 0 °C under N_2. After the addition was complete, then reaction mixture was allowed to warm to room temperature and then stirred for an additional 12 hr. After completion of the reaction, the reaction mixture was concentrated and then purified by column chromatography (8:2

EtOAc/Petroleum Ether) to yield **L2** (255 mg, 39%). Elemental analysis : Found: C, 56.44; H, 6.31; N, 19.140. Calc. for $C_{17}H_{23}N_5O_4$: C, 56.5; H, 6.37; N, 19.39%. IR (KBr, ν_{max}/cm^{-1}): 3348(s, NH), 3245 (s, NH), 1711 (s, CO), 1652 (s, CO). ^{1}H NMR δ_H (200 MHz; CD_3OD): 9.11 (s, 2 H, NH), 7.99 (s, 2 H, NH), 7.62 (dd, 2 H, J_1 = 3.5 Hz, J_2 = 6.1 Hz, Ph), 7.21 (dd, 2 H, J_1 = 3.6 Hz, J_2 = 6.0 Hz, Ph), 3.00 (s, 3 H, CH_3), 1.54 (s, 12 H, CH_3). ^{13}C NMR; δ_C (d_6 DMSO 200 MHz,): 173.6, 156.6, 130.86, 125.6, 59.0, 31.8, 25.5 . ESI-MS (negative ion mode): *m/z* 360.3 ($M\text{-}H^+$, 100%).

Synthesis of *$(Et_4N)_2[Fe^{III}(biuret\text{-}amide)]$* (**1**)

To a solution of compound **L2** (50 mg, 0.138 mmol) in 10 ml of dry THF was added n-BuLi (0.4 ml of 1.4 M solution in hexane, 0.567 mmoles, 4.1 eq) at 0 °C under Ar. Solid anhydrous $FeCl_2$ (21.1 mg, 0.166 mmoles,1.2 eq) was then added as a solid into this solution under positive argon flow. The reaction was allowed to proceed under Ar at room temperature for 12 hours after which it was opened to air to yield a dark orange-brown precipitate. The precipitate was filtered through a frit and was dissolved in methanol to afford an orange solution. The solution (5 ml) containing the complex was loaded onto a cationic ion-exchange resin (Amberlite-120) column that had been presaturated with $[Et_4N]^+$. The orange band was eluted with methanol and the solvent was removed under reduced pressure to yield a red-orange solid**.** Further purification was achieved by column chromatography using basic alumina with CH_2Cl_2:MeOH = 99:1 as the eluent. X-ray diffracting quality crystals were obtained by slow vapor diffusion of diethyl ether into the solution of the complex in acetonitrile. Yield : 60 mg (79%). Elemental analysis: Found: C, 55.71; H, 8.14; N,13.688%. Calc. for $C_{33}H_{59}N_7ClFeO_4$: C, 55.85; H, 8.32; N, 13.820. UV-VIS: $\lambda_{max}(H_2O)$/nm; 353 ($\varepsilon/dm^3\ mol^{-1}\ cm^{-1}$, 5164), IR (KBr, ν_{max}/cm^{-1}): 1601(s, CO),1556(s, CO),1531(s, CO) .ESI-MS (negative ion mode): *m/z 413.1*($M\text{-}H^+$, 100%).

Kinetics of Orange ll bleaching

Stock solutions of H_2O_2 (0.15M) , Orange II (3 x 10^{-3} M), **1** (2 x 10^{-5} M) and **2** (2 x 10^{-5} M) were made in double distilled water. Concentration of H_2O_2 was calculated by dividing the UV absorbance at 240 nm by the characteristic molar extinction coefficient (ε = 43.6 $dm^3\ mol^{-1}\ cm^{-1}$). In a typical kinetic run, 10 µL each of Orange II and the appropriate catalyst (**1** or **2**) stock solution was added to 970 µL of 0.01M phosphate buffer (having the appropriate pH of 7, 9, and

11) in a 1ml quartz cuvette. H_2O_2 (10 µL, 0.15 M) was added to initiate the reaction and the progress of the reaction was monitored by the disappearance of the Orange II peak at 485 nm. The cell compartment was thermostatted at 25 ºC. Initial rates were calculated from the pH dependent extinction co-efficients of Orange II. The initial rates used to calculate the pseudo-first order rate constant for the bleaching of Orange II by **1** at pH 11 were measured in triplicate.

Phosphate buffer based demetalation

Stock solutions of **1** (17.3 mM), 0.1 M, 0.2 M, 0.3 M, 0.5 M phosphate buffer of pH 5 and 7 are prepared in double distilled water. For each run, a solution of **1** (10 µL, 17.3 mM) in water was added to the appropriate phosphate buffer (990 µL) in a 1 mL cuvette and the decrease in absorbance at 350 nm (λ_{max} for **1** in phosphate buffer) was monitored over time. The temperature of the reaction mixture was maintained at 25 ºC throughout the experiment.

Bronsted acid induced demetalation

The kinetics were monitored in kinetic mode of the spectrophotometer (Perkin-Elmer –λ35) using 1.00 cm quartz cell at 360 nm (one of the absorption peaks of complex **1**) in an thermostatted (25.0 ± 0.5 °C) cell housing. In all kinetic runs, concentration of **1** was kept constant at 0.173 mM and acid concentration was varied from 0.04 to 0.4 M using $HClO_4$. KPF_6 was used to maintain the ionic strength at 0.1 M in the solution. For each set, solution pH was measured with a pH meter (LABINDIA, PICO$^+$) with calibrated electrode. The pseudo first order rate constants (k_{obs}) were calculated from the initial rates and plotted against [H^+] in **Figure S1** as has been shown before for acid catalyzed demetalation reaction of complex **2**.[3] All solutions were made using deionized water.

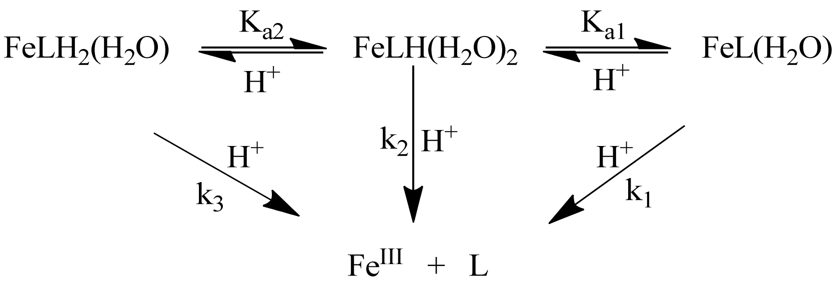

L = Biuret-amide macrocyclic ligand

Scheme S2: Proposed mechanism of acid induced demetalation

According to the Scheme S2, the rate law is,

$$k_{obs} = \frac{k_1K_{a1}K_{a2}[H^+] + k_2K_{a2}[H^+]^2 + k_3[H^+]^3}{K_{a1}K_{a2} + K_{a2}[H^+] + [H^+]^2}$$

$$= k_1^*[H^+] + k_2^*[H^+]^2 + k_3^*[H^+]^3 \qquad (1)$$

k_{obs} vs. $[H^+]$ plot (**Figure S1**) results were best fitted by using: $k_{obs} = k_1^*[H^+] + k_3^*[H^+]^3$ as has been described before.[3] Adding the second order $k_2^*[H^+]^2$ term did not improve the fit.

Table S1: Kinetic parameters of **1** in comparision with **2** in terms of acid catalysed demetalation

Catalyst	k_1^{*b}/ $M^{-1}s^{-1}$	k_3^{*b}/ $M^{-3}s^{-1}$
(**1**)[a]	(3.7 ± 0.5) x 10^{-3}	(1.04 ± 0.04) x 10^{-1}
(**2**)[3]	(2.2 ± 0.7)	(6.7 ± 0.2) x 10^{5}

[a] [**1**], [**2**] = 0.173 mM, $[H^+]$ = (0.04 - 0.4) M, I = 0.1 M(KPF_6) and T = 25.0±0.5 °C

[b] k_1^* corresponds to mild acidic while k_3^* stands for strong acidic condition

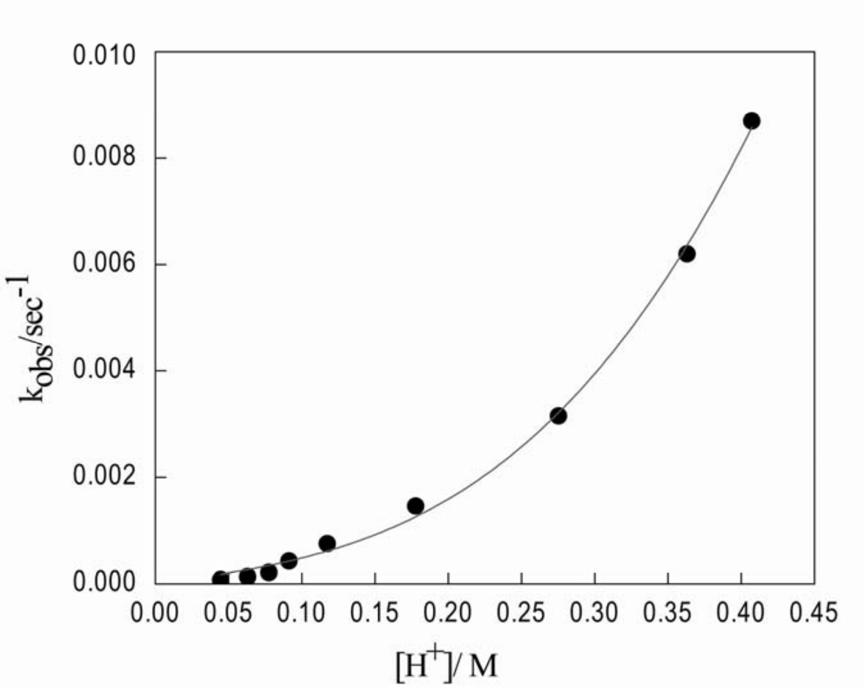

Figure S1: Plot of k_{obs} vs. [H$^+$] for acid induced demetalation of **1** (0.173 mM) in 0.1 M KPF_6 at 25.0 ± 0.5 °C. The solid line was drawn according to the rate law derived from Scheme S2. Adding the second order k_2*[H$^+$]^2 term did not improve the fit.

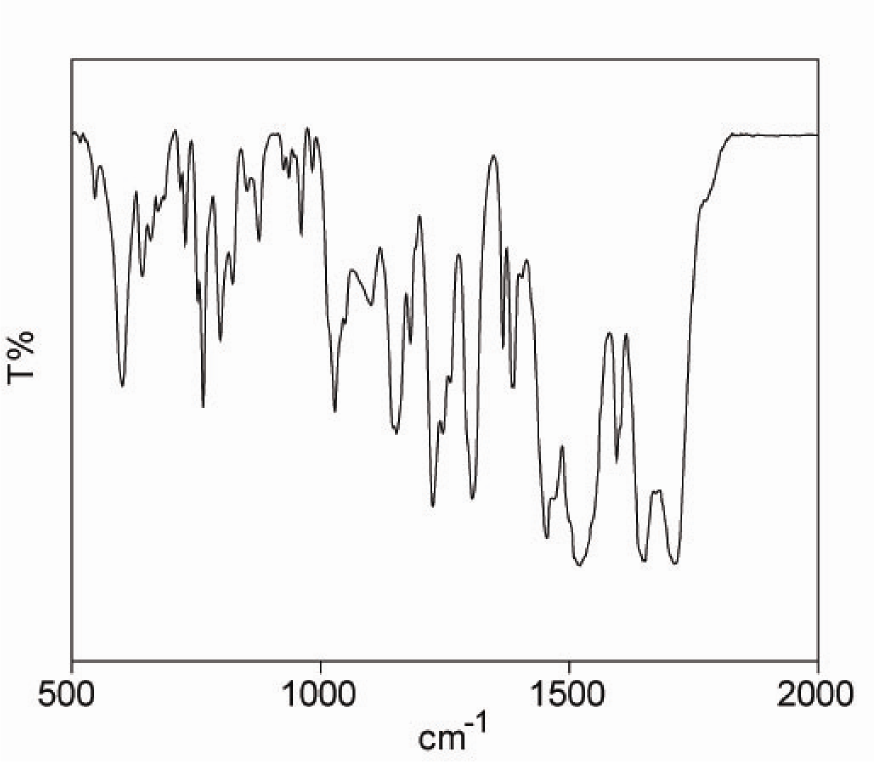

Figure S2 : FT-IR spectra of biuret-amide macrocyclic ligand(**L2**)

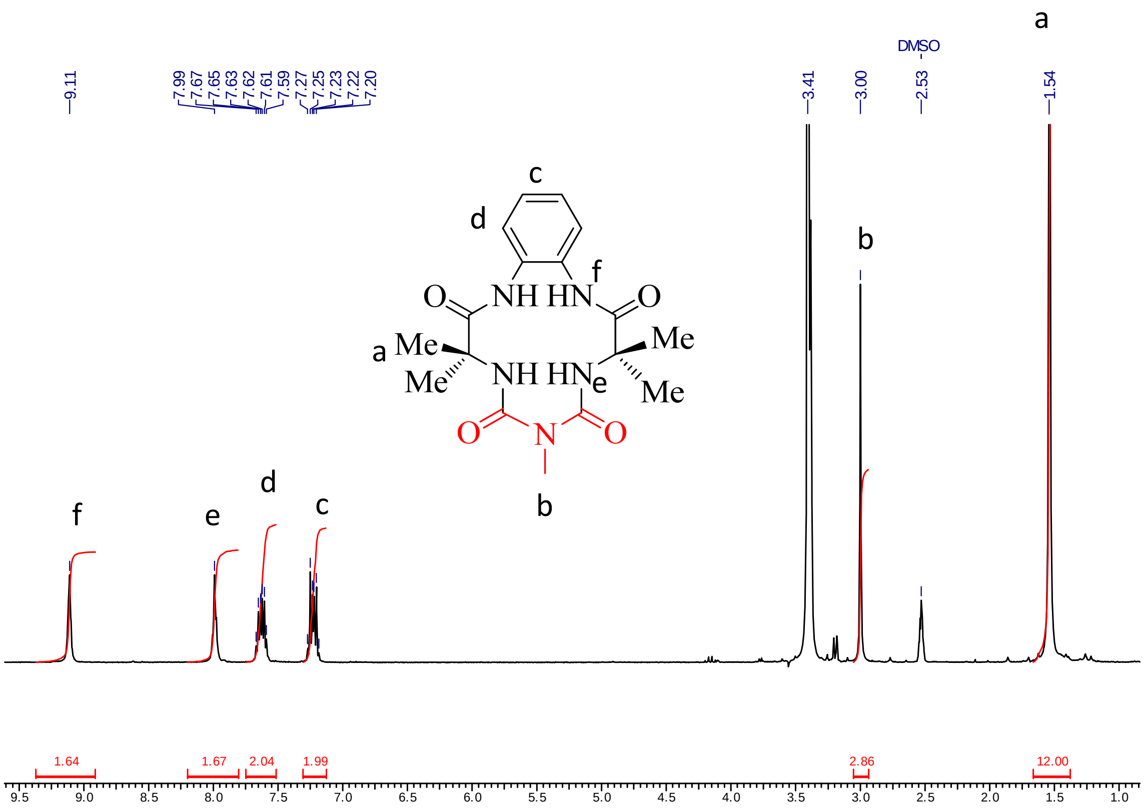

Figure S3 : ^{1}H NMR of biuret-amide macrocyclic ligand (**L2**)

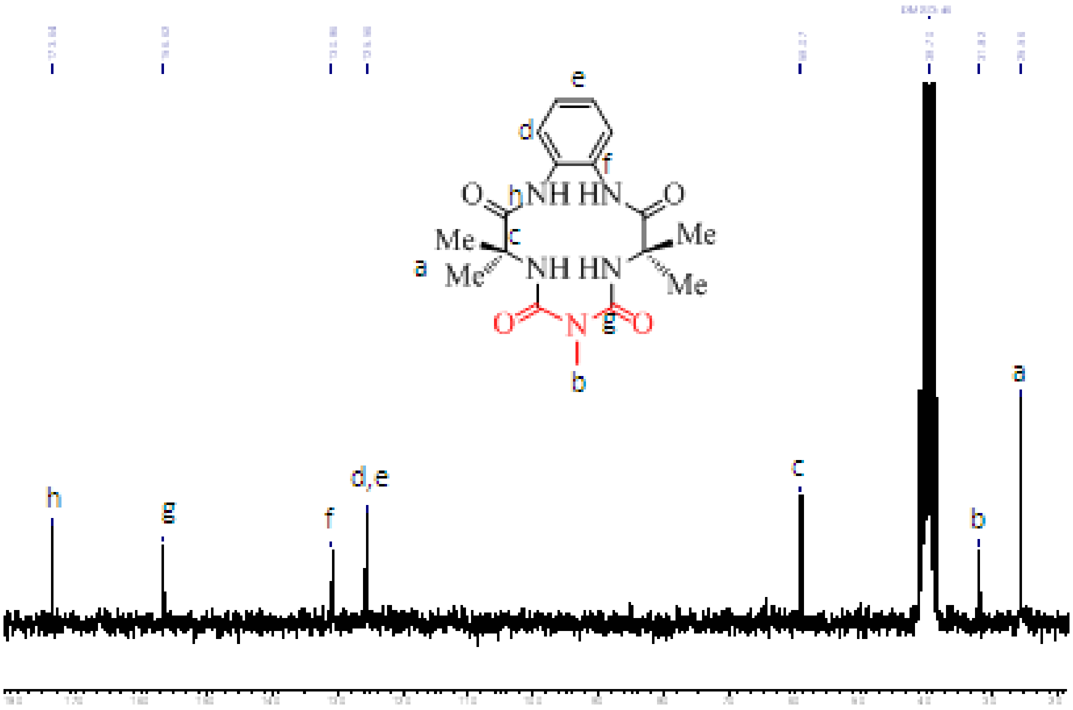

Figure S4 : ^{13}C NMR of biuret-amide macrocyclic ligand (**L2**)

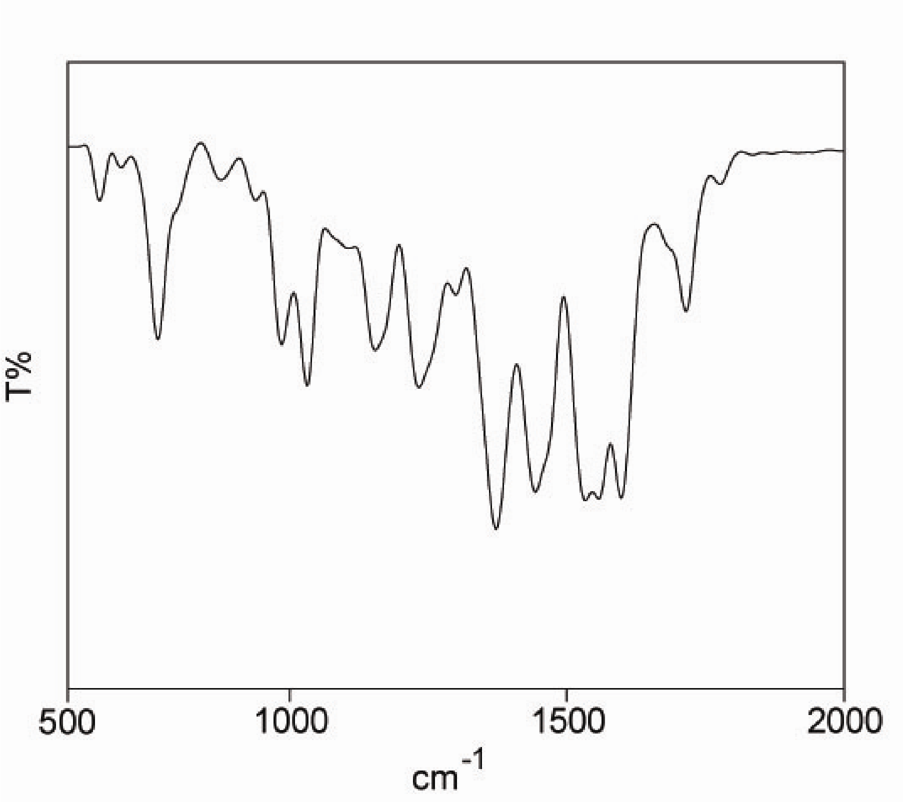

Figure S5: FT-IR Spectra of $(Et_4N)_2[Fe^{III}(\text{biuret-amide})]$(**1**)

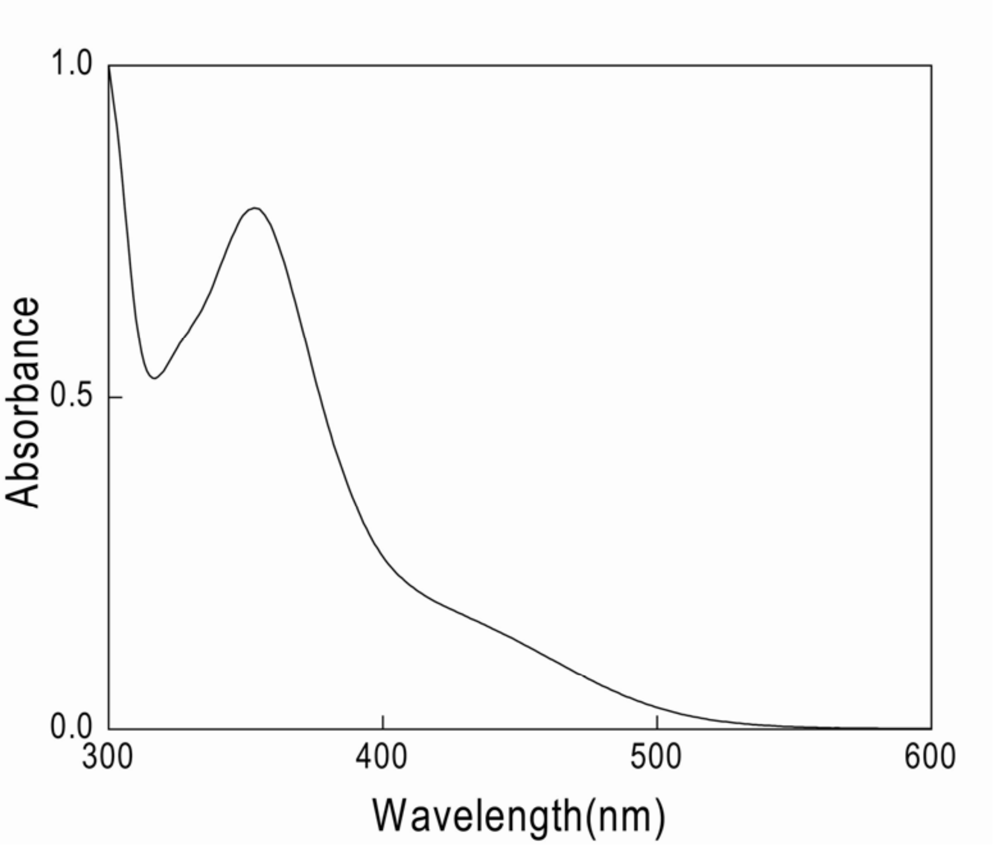

Figure S6: UV-Visible spectra of $(Et_4N)_2[Fe^{III}(biuret\text{-}amide)]$(**1**) in water (0.138 mM)

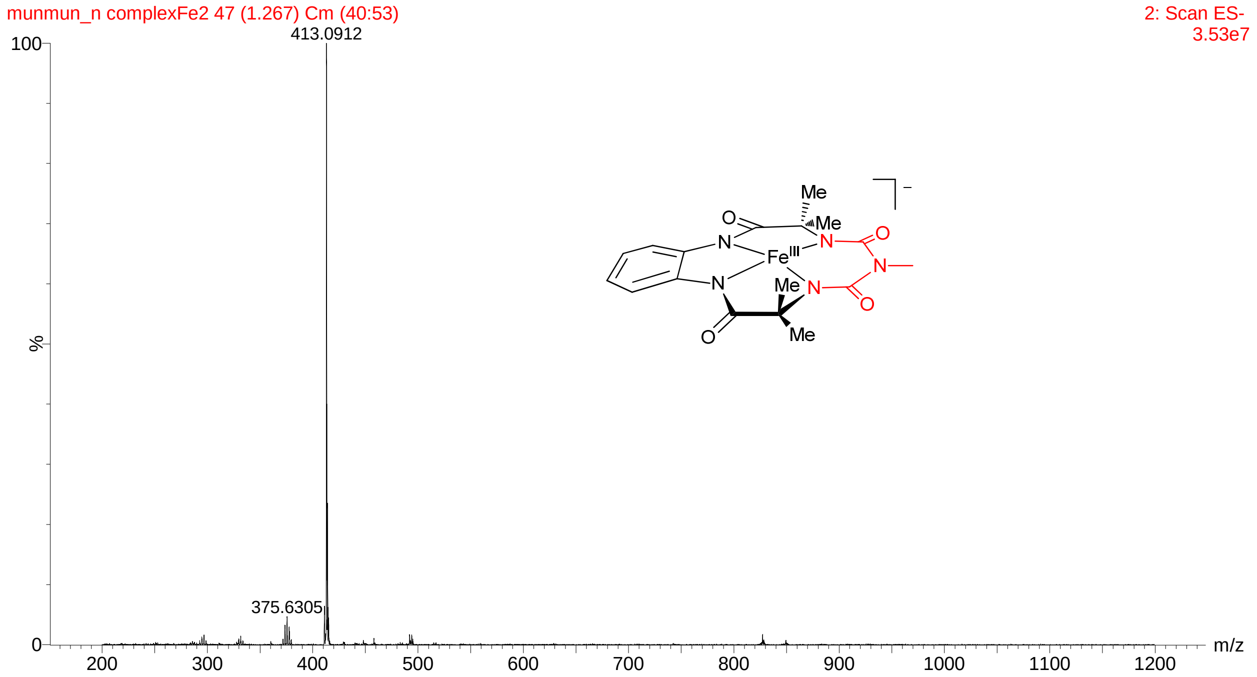

Figure S7: ESI-MS of a solution of $(Et_4N)_2[Fe^{III}(\text{biuret-amide})]$(**1**) in methanol (m/z 413). The axial chloro ligand is not observed as this ligand is labile and gets dissociated under the conditions of the mass spectrometry experiment.

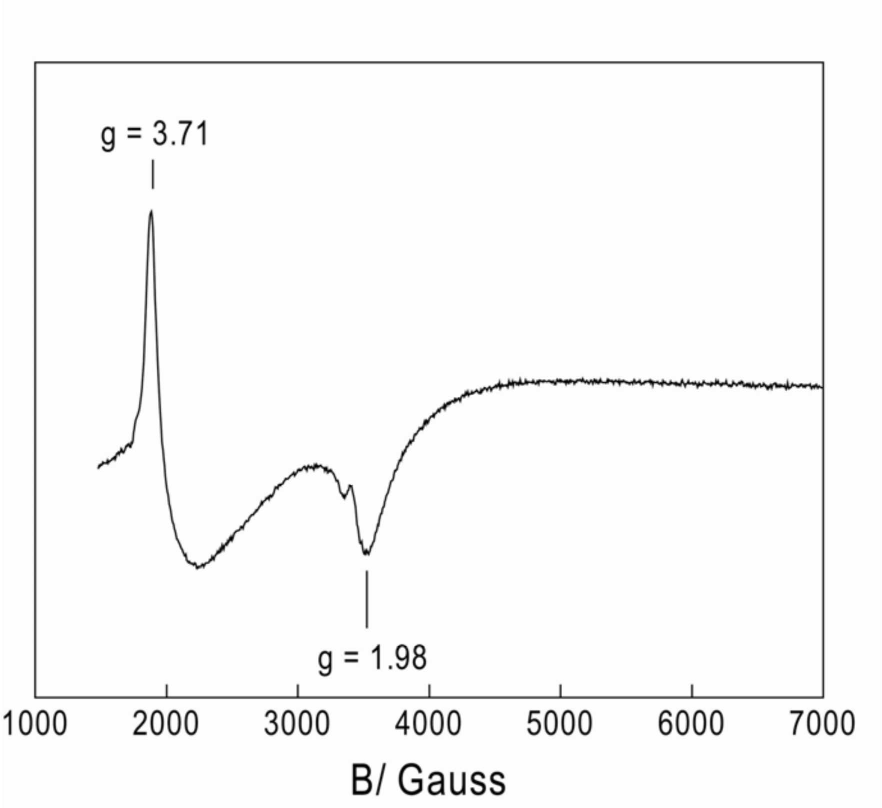

Figure S8: X-band EPR spectrum of $(Et_4N)_2[Fe^{III}$(biuret-amide)](**1**) solid at 298 K

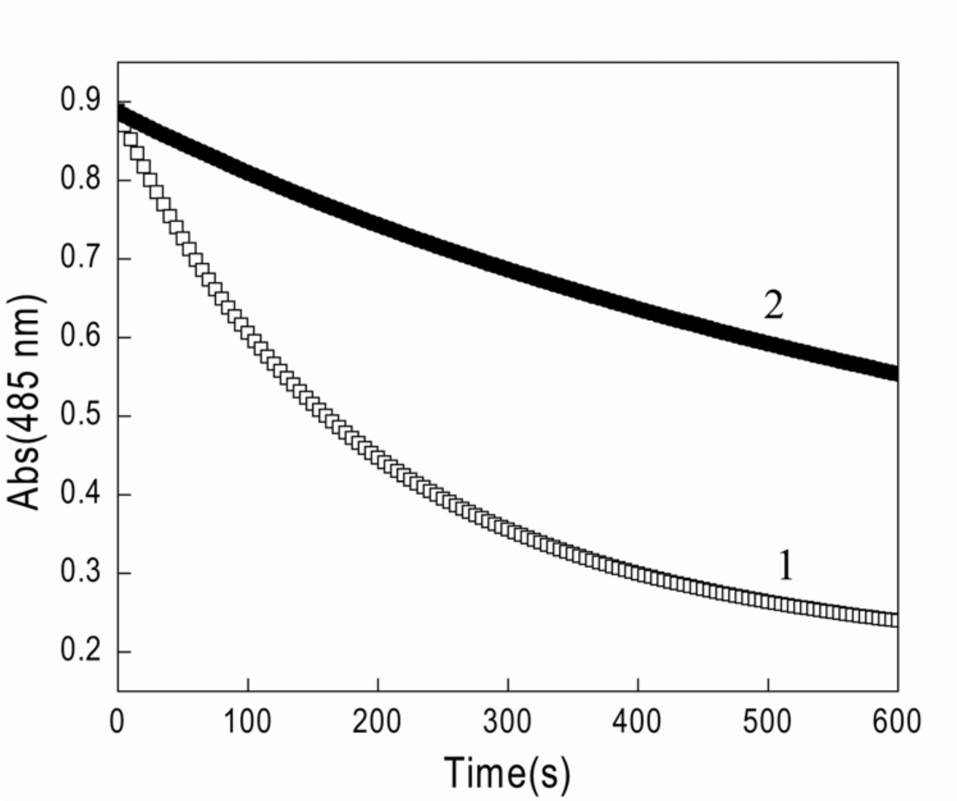

Figure S9: Comparative Orange II bleaching by H_2O_2 at pH 7 for **1** and **2**. [Catalyst] = 2 x 10^{-7} M, [H_2O_2] = 0.0015 M, [Orange II] = 4 x 10^{-5} M; 0.01 M phosphate buffer, 25 °C

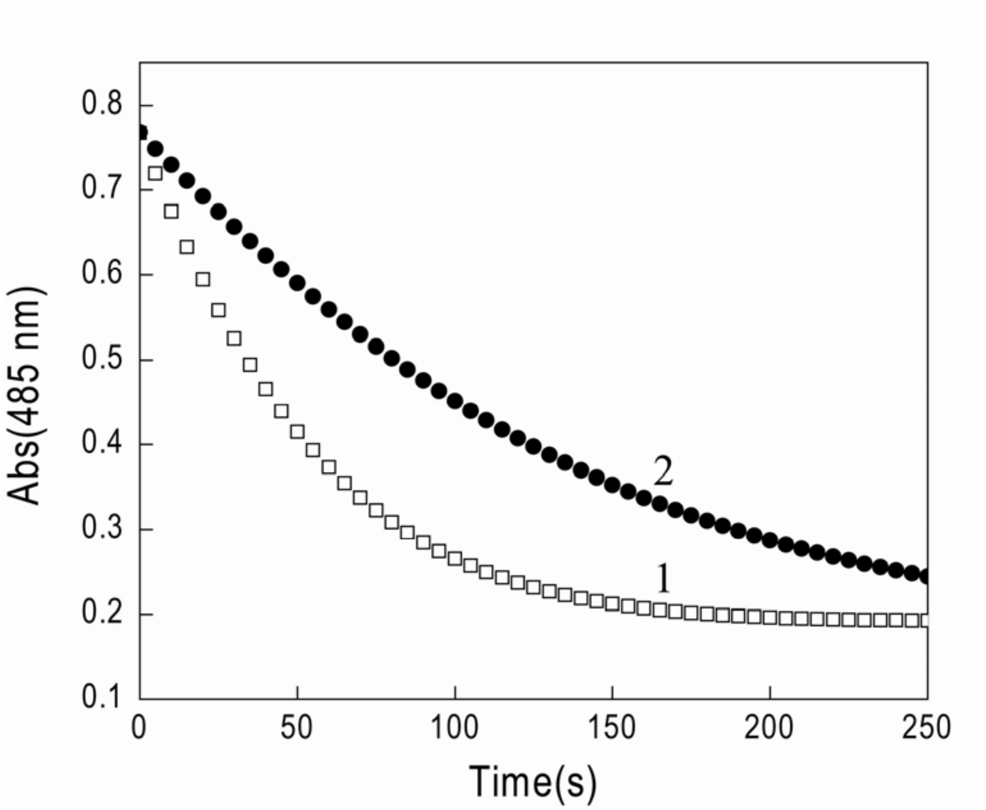

Figure S10: Comparative Orange II bleaching by H_2O_2 at pH 9 for **1** and **2**.[Catalyst] = 2 x 10^{-7} M, [H_2O_2] = 0.0015 M, [Orange II] = 4 x 10^{-5} M; 0.01 M phosphate buffer, 25 °C

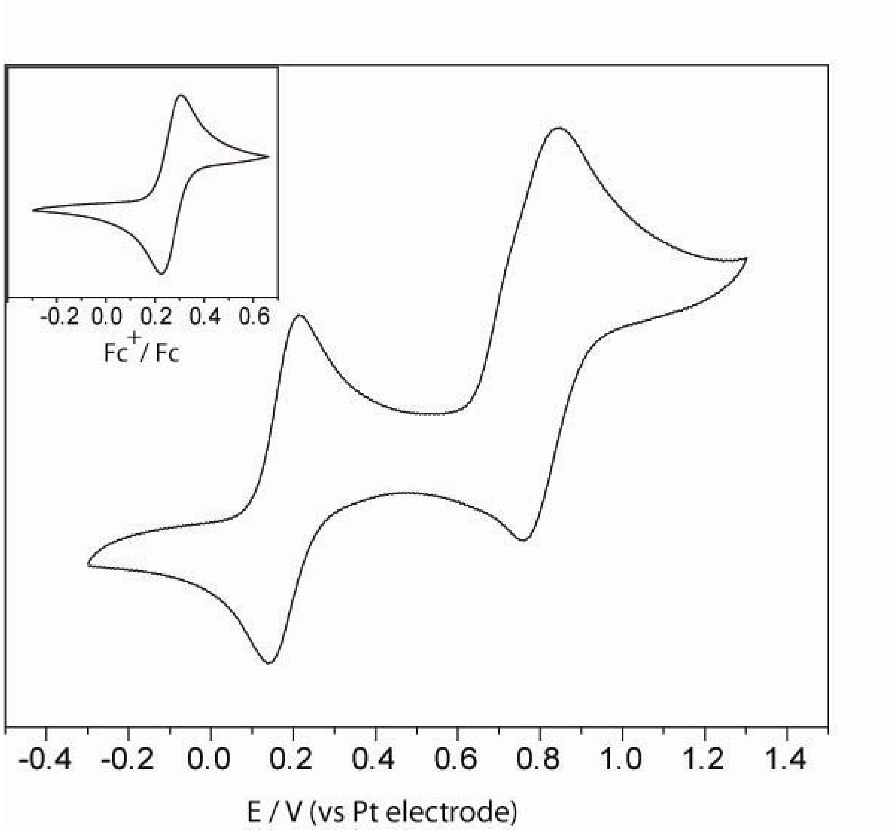

Figure S11: Cyclic voltammogram of $(Et_4N)_2[Fe^{III}$(biuret-amide)](**1**) vs Pt wire in CH_3CN (0.1 M n-Bu_4NPF_6, sweep rate 100 mV/sec). The Fc^+/Fc couple under the same experimental condition is shown in inset.

Single crystal X-ray diffraction data collection, structure solution and refinement procedures.

General Data Collection and Refinement Procedures

Single crystal data were collected on a Bruker SMART APEX three circle diffractometer equipped with a CCD area detector and operated at 1500 W power (50 kV, 30 mA) to generate Mo Kα radiation (λ=0.71073 Å). The incident X-ray beam was focused and monochromated using Bruker Excalibur Gobel mirror optics. Suitable crystal of **1** reported in the paper were mounted on nylon CryoLoops (Hampton Research) with Paraton-N (Hampton Research).

Initial scans of each specimen were performed to obtain preliminary unit cell parameters and to assess the mosaicity (breadth of spots between frames) of the crystal to select the required frame width for data collection. In every case frame widths of 0.5° were judged to be appropriate and full hemispheres of data were collected using the *Bruker SMART*[4] software suite. Following data collection, reflections were sampled from all regions of the Ewald sphere to redetermine unit cell parameters for data integration and to check for rotational twinning using CELL_NOW[5]. In no data collection was evidence for crystal decay encountered. Following exhaustive review of the collected frames the resolution of the dataset was judged. Data were integrated using Bruker SAINT[6] software with a narrow frame algorithm and a 0.400 fractional lower limit of average intensity. Data were subsequently corrected for absorption by the program SADABS[7]. The space group determinations and tests for merohedral twinning were carried out using *XPREP*[6]. In all cases, the highest possible space group was chosen.

Crystal structure of **1** was solved by direct methods and refined using the *SHELXTL 97*[8] software suite. Atoms were located from iterative examination of difference F-maps following least squares refinements of the earlier models. Final model was refined anisotropically (if the number of data permitted) until full convergence was achieved. Hydrogen atoms were placed in calculated positions (C-H = 0.93 Å) and included as riding atoms with isotropic displacement parameters 1.2-1.5 times U_{eq} of the attached C atoms. Data were collected at 200(2) K. This lower temperature was considered to be optimal for obtaining the best data. Crystal structure of **1** was examined using the *Adsym* subroutine of PLATON[8] to assure that no additional symmetry could be applied to the model. ORTEP diagram is displayed at the 50% probability level.

A colorless prismatic crystal ($0.25 \times 0.20 \times 0.18$ mm^3) of **1** was placed in a 0.7 mm diameter nylon CryoLoops (Hampton Research) with Paraton-N (Hampton Research). The loop was mounted on a SMART APEX three circle diffractometer. A total of 82276 reflections were collected of which 4743 were unique and 2863 of these were greater than $2\sigma(I)$. The range of θ was from 2.28 to 19.11°. All non-hydrogen atoms were refined anisotropically. **1** contains half ligand molecule in the asymmetric unit. It should be noted that other supporting characterization data (*vide infra Synthesis*) are consistent with the crystal structure. Final full matrix least-squares refinement on F^2 converged to $R_1 = 0.0551$ and $wR_2 = 0.1765$(all data) with GOF = 0.905. Table S2 contains crystallographic data for **1**.

Table S2: Crystal data and structure refinement for $[Et_4N]_2[Fe^{III}$(biuret-amide)] (**1**)

Empirical formula	C33 H39 Cl Fe N7 O4
Formula weight	689.01
Temperature	296(2) K
Wavelength	0.71073 Å
Crystal system	Tetragonal
Space group	*P42/mbc*
	a = 22.169(17) Å α = 90°
Unit cell dimensions	*b* = 22.169(17) Å β = 90°
	c = 14.93(2) Å γ = 90°
Volume	7338(13)
Z	8
Density (calculated)	1.247
Absorption coefficient	0.528
F(000)	2888
Crystal size	0.30 × 0.20 × 0.15 mm^3
Theta range for data collection	10.42– 18.13
Index ranges	-29<= h <= 29, -29<= k <= 29, -19<= l <= 19
Reflections collected	81929
Independent reflections	4711
Completeness to theta = 26.02°	98.7 %
Absorption correction	Semi-empirical from equivalents
Refinement method	Full-matrix least-squares on F^2
Data / restraints / parameters	4711 / 0 / 242
Goodness-of-fit on F^2	1.019
Final R indices [I>2sigma(I)]	R_1 = 0.0660, wR_2 = 0.1985
R indices (all data)	R_1 = 0.1108, wR_2 = 0.2182
Largest diff. peak and hole	1.662 and -0.490 e.Å^{-3}

Note: The carbon atoms of one the tetraethyl ammonium cation is disorder. So we could not locate or fixed so we refined the structure without adding any hydrogen atoms to it.

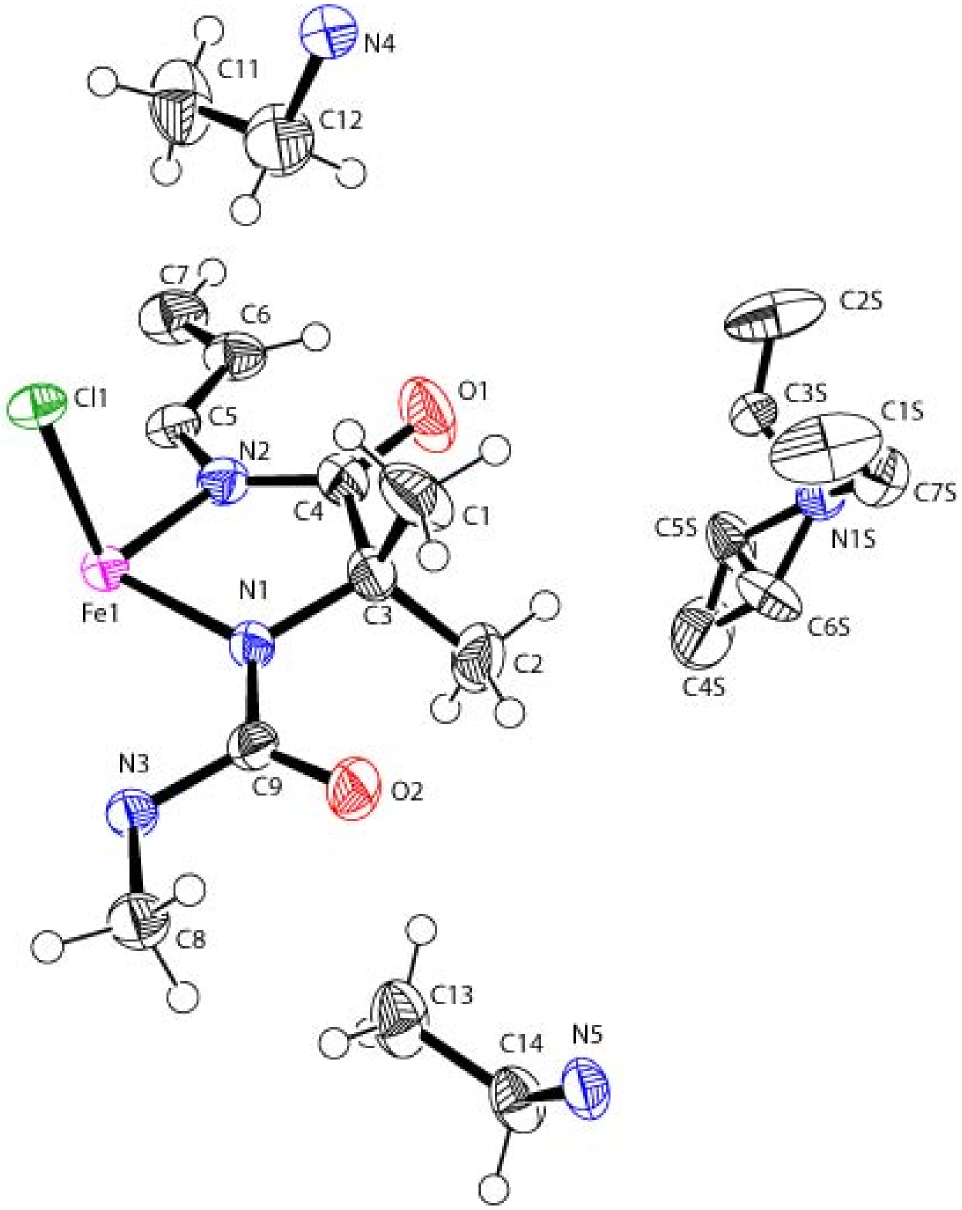

Figure S12: Ortep diagram of $[Et_4N]_2[Fe^{III}$(biuret-amide)] (**1**) in asymmetric unit. The complex $(Et_4N)_2[Fe^{III}$(biuret-amide)] crystallizes in tetragonal crystal system (space group, $P4_2/mbc$). The asymmetric unit of $(Et_4N)_2[Fe^{III}$(biuret-amide)] contains one half $[Fe^{III}$(biuret-amide)] molecule (with mirror symmetry, no disorder; 50% occupancy of Fe and Cl), and two one quarter (25%

occupancy of nitrogen) and one half (50% occupancy of nitrogen) Et_4N molecules. [Fe^{III}(biuret-amide)] molecule occupies a mirror symmetry where half [Fe^{III}(biuret-amide)] molecule is related to the other half by mirror.

Comparison of the X-ray data with the Elemental analysis

The complex $(Et_4N)_2$[Fe^{III}(biuret-amide)] crystallizes in tetragonal crystal system (space group, $P4_2/mbc$). The asymmetric unit of $(Et_4N)_2$[Fe^{III}(biuret-amide)] contains one half [Fe^{III}(biuret-amide)] molecule (with mirror symmetry, no disorder; 50% occupancy of Fe and Cl), and two one quarter (25% occupecy of nitrogen) and one half (50% occupecy of nitrogen) Et_4N molecules. [Fe^{III}(biuret-amide)] molecule occupies a mirror symmetry where half [Fe^{III}(biuret-amide)] molecule is related to the other half by mirror. If we calculate the charge of the asymmetric unit considering Fe is in +3 oxidation stage.
Fe (50%) = (+)1.5
Two one quarter Et_4N molecules (25% occupecy of nitrogen)= (+)0.25+(+)0.25=(+)0.5
One half Et_4N molecules (50% occupecy of nitrogen)= (+)0.5
Total (+) charge of the asymmetric unit is (+)1.5+(+)0.5+(+)0.5= (+)2.5

Similarly for the (-) ve charge
Cl(50%) = (-)0.5
Two nitrogen (100%) from the (biuret-amide) moiety = (-)2.0
Total (+) charge of the asymmetric unit is (-)0.5+(-)2.0= (-)2.5

Hence we could conclude Fe in the $(Et_4N)_2$[Fe^{III}(biuret-amide)] complex is indeed in +3 oxidation state. This is clearly indicative from the inspection of the CIF file (CCDC entry no. 812577). The sum formula for this revised cif is $C_{33}H_{39}Cl_1Fe_1N_7O_4$ and thus a molecular weight of M = 689.17 g/mol. We have not added the 20 hydrogen's of the disordered Et_4N molecule.

The charge on the Fe mentioned above is calculated based on the contents of the asymmetric unit or the content of the unit cell. In either cases the we have concluded that the oxidation state of the Fe here is +3.

The Elemental analysis data is as follows: Found: C, 55.71; H, 8.14; N,13.688%. Calc. for $C_{33}H_{59}N_7ClFeO_4$: C, 55.85; H, 8.32; N, 13.820

The current elemental analysis matches exactly with the X-ray crystal structure. The sum formula for this revised cif is $C_{33}H_{39}Cl_1Fe_1N_7O_4$ and thus a molecular weight of M = 689.17 g/mol. We have not added the 20 hydrogen's of the disordered Et_4N molecule. The formula of the $(Et_4N)_2$[Fe^{III}(biuret-amide)] hence derived from the crystal structure should be $C_{33}H_{59}Cl_1Fe_1N_7O_4$.

Table S3 : Selected bond lengths

Atoms	Bond Lengths(A)
C1-N5	1.447(5)
C6-O2	1.245(4)
C6-N2	1.349(4)
C6-N5	1.416(3)
Cl-Fe1	2.3948(11)
Fe1-N2	1.879(2)
Fe1-N1	1.881(3)
Fe1-N5	3.149

Table S4 : Selected bond angles

Atoms	Bond Angles(o)
O2-C6-N2	124.5(3)
O2-C6-N5	116.8(3)
N2-Fe1-N2	95.33(15)
N2-Fe1-N1	152.11(12)
N2-Fe1-N1	84.22(11)
N2-Fe1-N1	84.21(11)
N1-Fe1-N1	152.10(12)
N1-Fe1-N1	83.51(16)
N2-Fe1-Cl1	104.60(8)
N2-Fe1-Cl1	104.60(8)
N1-Fe1-Cl1	102.47(8)
N1-Fe1-Cl1	102.47(8)
C6-N2-C4	119.2(2)
C6-N2-Fe1	125.8(2)
C6-N5-C6	130.2(3)
C6-N5-C1	114.66(17)
C6-N5-C1	114.66(17)

Supplemental Information References

1. Armarego, W.L.F., Chai, C.L.L. *Purification of Laboratory Chemicals, 5th ed*. Elsevier Science: Burlington, MA, 2003
2. A. Ghosh, P. Ramidi, S. Pulla, S. Z. Sullivan, S. L. Collom, Y. Gartia, P. Munshi, A. S. Biris, B. C. Noll, B. C. Berry, *Catalysis Letters*,2010, **137**, 1.
3. A. Ghosh, A. D. Ryabov, S. M. Mayer, D. C. Horner, D. E. Prasuhn, S. Sen Gupta, L. Vuocolo, C. Culver, M. P.Hendrich, C. F.Rickard, R. Norman, C. Horwitz, T. J. Collins, *Journal of the American Chemical Society,* 2003*,* ***125****, 41, 12379.*
4. Bruker (2005). *APEX2*. Version 5.053. Bruker AXS Inc., Madison,Wisconsin, USA.
5. G. M. Sheldrick, (2004). *CELL_NOW*. University of Göttingen, Germany. Steiner, Th. (1998). *Acta Cryst*. **B54**, 456.
6. Bruker (2004). *SAINT-Plus* (Version 7.03). Bruker AXS Inc., Madison, Wisconsin, USA.
7. G. M. Sheldrick, (2002). *SADABS* (Version 2.03) and *TWINABS* (Version 1.02).University of Göttingen, Germany.
8. G. M. Sheldrick, (1997). *SHELXS ‘97* and *SHELXL ‘97*. University of Göttingen, Germany.